JOC Article

A Joint Experimental and Theoretical Study of the Palladium-Catalyzed Electrophilic Allylation of Aldehydes

Olivier Piechaczyk, Thibault Cantat, Nicolas Mézailles, and Pascal Le Floch*

Laboratoire "Hétéroéléments et Coordination", École Polytechnique, CNRS, 91128, Palaiseau, France

lefloch@poly.polytechnique.fr

Received March 6, 2007

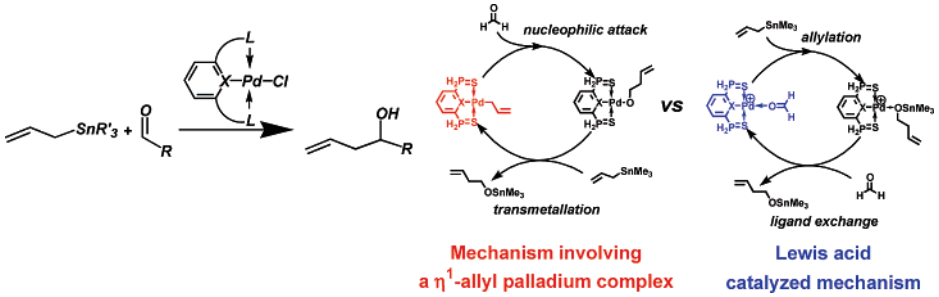

Palladium-catalyzed electrophilic allylation of aldehydes with allylstannanes has been proposed in the literature as a model reaction illustrating the potential of nucleophilic η^1-allyl palladium pincer complexes to promote new catalytic processes. This reaction was studied by a joint experimental and theoretical approach. It was shown that pincer palladium complexes featuring a S∼P∼S and a S∼C∼S tridentate ligand are efficient catalysts for this reaction. The full mechanism of this transformation was studied in detail by means of DFT calculations. Two pathways were explored: the commonly proposed mechanism involving η^1-allyl palladium intermediates and a Lewis acid promoted mechanism. Both of these mechanisms were compared to the direct transformation that was shown experimentally to occur under mild conditions. The mechanism involving an η^1-allyl palladium intermediate has been discarded on energetic grounds, the nucleophilic attack and the transmetalation step being more energetically demanding than the direct reaction between allyltin and the aldehyde. On the other hand, a mechanism where the palladium acts as a Lewis acid proved to be fully consistent with all experimental and theoretical results. This mechanism involves (L∼X∼L)Pd^+ species which activate the aldehyde moiety toward nucleophilic attack.

Introduction

Transition-metal complexes have demonstrated their high potential for the formation of carbon−carbon and carbon-heteroatom bonds. Among these, allylic alkylations have been widely studied since they allow coupling at an sp^3-hybridized carbon atom. Although various metals have been shown to catalyze these processes,[1−9] palladium complexes stand out as the most efficient catalysts.[3,5,10] The principle of these couplings relies on the transient formation of a cationic η^3-allyl palladium complex that undergoes a nucleophilic attack on the activated allyl moiety. The η^3-allyl palladium complex is then regenerated through oxidative addition of the palladium(0) species to the allylic substrate (Scheme 1, A).

The precise understanding of the mechanism of this nucleophilic allylation has been the subject of numerous studies over

* Author to whom correspondence should be addressed. Tel: 33-1-69-33-45-70. Fax: 33-1-69-33-39-90.

(1) Fuji, K.; Kinoshita, N.; Tanaka, K.; Kawabata, T. *Chem. Commun.* **1999**, 2289−2290.
(2) Ohmura, T.; Hartwig, J. F. *J. Am. Chem. Soc.* **2002**, *124*, 15164−15165.
(3) Trost, B. M.; VanVranken, D. L. *Chem. Rev.* **1996**, *96*, 395−422.
(4) Trost, B. M.; Toste, F. D.; Pinkerton, A. B. *Chem. Rev.* **2001**, *101*, 2067−2096.
(5) Trost, B. M.; Crawley, M. L. *Chem. Rev.* **2003**, *103*, 2921−2943.
(6) Lopez, F.; Ohmura, T.; Hartwig, J. F. *J. Am. Chem. Soc.* **2003**, *125*, 3426−3427.
(7) Evans, P. A.; Leahy, D. K. *J. Am. Chem. Soc.* **2000**, *122*, 5012−5013.
(8) Ariafard, A.; Lin, Z. Y. *Organometallics* **2005**, *24*, 3800−3806.
(9) Kiener, C. A.; Shu, C. T.; Incarvito, C.; Hartwig, J. F. *J. Am. Chem. Soc.* **2003**, *125*, 14272−14273.
(10) Tamaru, Y. *Eur. J. Org. Chem.* **2005**, 2647−2656.

10.1021/jo070467t CCC: $37.00
Published on Web 04/21/2007

SCHEME 1. General Mechanism of the Palladium-Catalyzed Nucleophilic Allylation Process (A) and Proposed Mechanism for the Electrophilic Allylation Process (B)

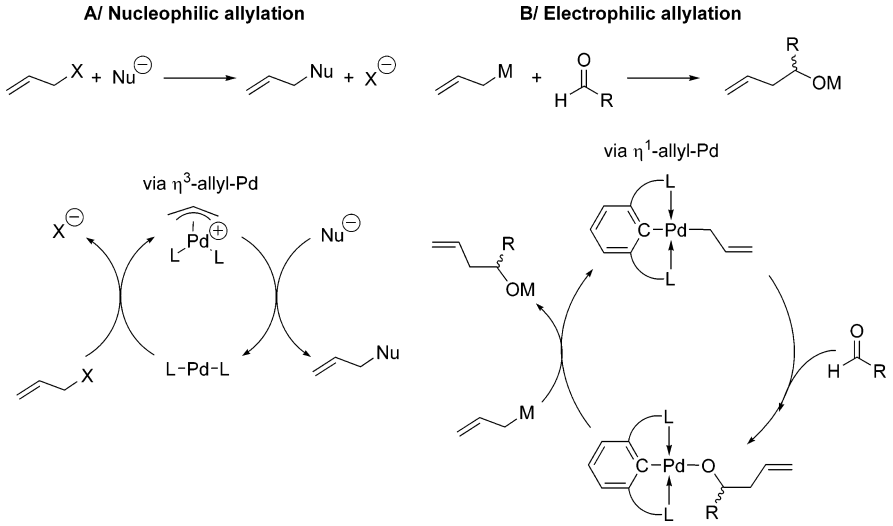

SCHEME 2. Catalysts Proposed for the Allylation of Aldehydes with Allyltributyltin

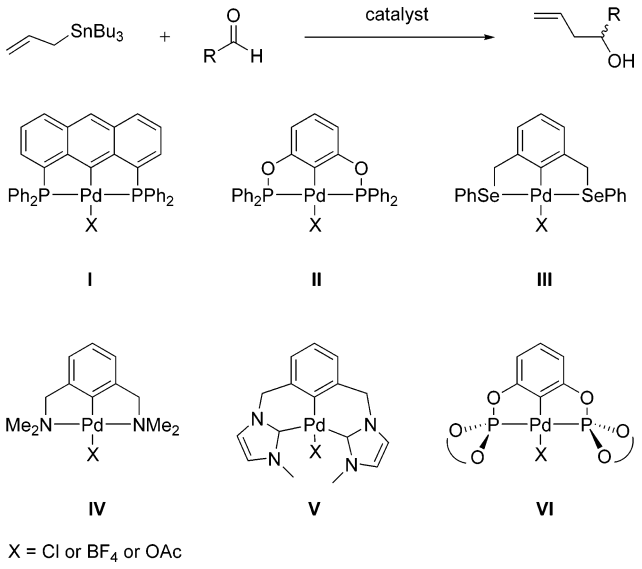

the last two decades.[11−20] Being key intermediates, the allyl palladium complexes were thoroughly investigated both in terms of synthesis and chemical reactivity.[21−27] Following these studies, η^1-allyl palladium complexes have been recently shown to exhibit a nucleophilic character.[28−33] The umpolung character of the η^1-allyl moiety has attracted much attention since it can promote new types of catalytic allylations and thus widen the synthetic scope of allyl palladium complexes. In fact, nucleophilic η^1-allyl palladium species have been proposed for the catalytic allylation of electrophilic substrates such as carbonyl compounds and imines (Scheme 1, B).[29−32]

In 2003, Szabó and co-workers reported on interesting advances in the promotion of new allylation processes by using pincer palladium complexes in the catalyzed conversion of aldehydes into homoallylalcohols through reaction with allylstannanes (Scheme 2).[34] Tridentate pincer ligands were chosen because they occupy three of the four coordination sites of a square planar Pd^{II} complex and therefore impose an η^1-coordination mode of the allyl fragment. Moreover, contrary to bis-allyl palladium complexes, the resulting η^1-allyl palladium complexes cannot undergo a reductive elimination that would release the allyl fragment (allyl−allyl coupling).[29] They therefore possess an enhanced stability. Results of these studies led the authors to propose a mechanism which involves the transient formation of an η^1-allyl palladium intermediate which further undergoes an electrophilic attack from the aldehyde. A subse-

(11) Amatore, C.; Gamez, S.; Jutand, A. *Chem.-Eur. J.* **2001**, *7*, 1273−1280.
(12) Amatore, C.; Bahsoun, A. A.; Jutand, A.; Mensah, L.; Meyer, G.; Ricard, L. *Organometallics* **2005**, *24*, 1569−1577.
(13) Amatore, C.; Jutand, A.; Mensah, L.; Meyer, G.; Fiaud, J. C.; Legros, J. Y. *Eur. J. Org. Chem.* **2006**, 1185−1192.
(14) Backvall, J. E.; Nordberg, R. E.; Zetterberg, K.; Akermark, B. *Organometallics* **1983**, *2*, 1625−1629.
(15) Piechaczyk, O.; Thoumazet, C.; Jean, Y.; le Floch, P. *J. Am. Chem. Soc.* **2006**, *128*, 14306−14317.
(16) Cantat, T.; Genin, E.; Giroud, C.; Meyer, G.; Jutand, A. *J. Organomet. Chem.* **2003**, *687*, 365−376.
(17) Cantat, T.; Agenet, N.; Jutand, A.; Pleixats, R.; Moreno-Manas, M. *Eur. J. Org. Chem.* **2005**, 4277−4286.
(18) Sakaki, S.; Nishikawa, M.; Ohyoshi, A. *J. Am. Chem. Soc.* **1980**, *102*, 4062−4069.
(19) Ozawa, F.; Ishiyama, T.; Yamamoto, S.; Kawagishi, S.; Murakami, H.; Yoshifuji, M. *Organometallics* **2004**, *23*, 1698−1707.
(20) Tang, D. Y.; Luo, X. L.; Shen, W.; Li, M. *J. Mol. Struct. (THEOCHEM)* **2005**, *716*, 79−87.
(21) Braunstein, P.; Naud, F.; Dedieu, A.; Rohmer, M. M.; DeCian, A.; Rettig, S. J. *Organometallics* **2001**, *20*, 2966−2981.
(22) Ramdeehul, S.; Barloy, L.; Osborn, J. A.; DeCian, A.; Fischer, J. *Organometallics* **1996**, *15*, 5442−5444.
(23) Barloy, L.; Ramdeehul, S.; Osborn, J. A.; Carlotti, C.; Taulelle, F.; De Cian, A.; Fischer, J. *Eur. J. Inorg. Chem.* **2000**, 2523−2532.
(24) Braunstein, P.; Jing, Z. A.; Welter, R. *Dalton Trans.* **2003**, 507−509.
(25) Kollmar, M.; Helmchen, G. *Organometallics* **2002**, *21*, 4771−4775.
(26) Tsuji, J.; Takahash, H.; Morikawa, M. *Tetrahedron Lett.* **1965**, 4387.
(27) Consiglio, G.; Waymouth, R. M. *Chem. Rev.* **1989**, *89*, 257−276.
(28) Espinet, P.; Echavarren, A. M. *Angew. Chem., Int. Ed.* **2004**, *43*, 4704−4734.
(29) Nakamura, H.; Bao, M.; Yamamoto, Y. *Angew. Chem., Int. Ed.* **2001**, *40*, 3208.
(30) Szabo, K. J. *Chem. Eur. J.* **2000**, *6*, 4413−4421.
(31) Szabo, K. J. *Chem. Eur. J.* **2004**, *10*, 5269−5275.
(32) Wallner, O. A.; Szabo, K. J. *J. Org. Chem.* **2003**, *68*, 2934−2943.
(33) (a) Garcia-Iglesias, M.; Bunuel, E.; Cardenas, D. J. *Organometallics* **2006**, *25*, 3611−3618; (b) Pichierri, F.; Yamamoto, Y. *J. Org. Chem.* **2007**, *72*, 861−869.
(34) Solin, N.; Kjellgren, J.; Szabo, K. J. *Angew. Chem., Int. Ed.* **2003**, *42*, 3656−3658.

SCHEME 3. General Synthesis of S∼P∼S-Based Transition Metal Complexes

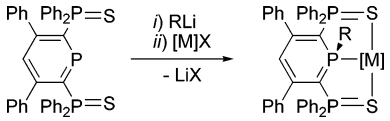

SCHEME 4. Catalytic Allylation of Aldehydes with Allyltributyltin

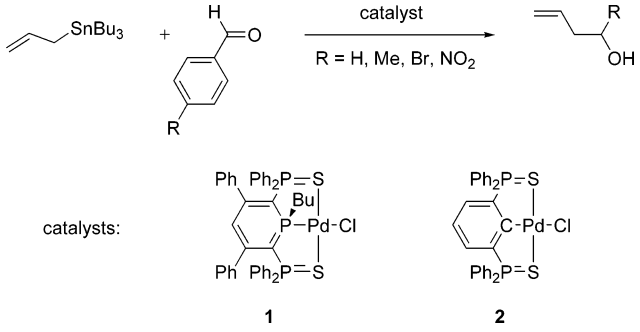

quent transmetalation step with allylstannanes or potassium allyltrifluoroborates was proposed to account for the reformation of the active η^1-allyl palladium species and the release of the desired product (Scheme 1B, M = SnR_3 or BF_3K).[34−38]

These two steps require different electronic properties at the metal center. Indeed an electron rich metal fragment would favor the nucleophilic attack of the η^1-allyl moiety while an electron deficient metal center would favor the transmetalation step.[35] Thus, a fine-tuning of the ligand is needed for the design of an efficient catalyst. Recently, several orthometalated palladium pincer complexes featuring a L∼C∼L skeleton (L = 2e donor ligand) have been tested in the catalytic allylation of aldehydes with allyltributyltin (Scheme 2). These catalysts exhibit different activities: whereas the more electron rich complexes **IV** and **V**,[35] which feature strong σ-donor ancillary ligands, display low activities, complexes **I**, **II**,[35] **III**[37] and **VI**,[38] with balanced electronic properties, proved to be much more efficient. The asymmetric version of this reaction has been lately reported, with chiral orthometalated phosphite ligands (catalyst **VI**). Although some elementary steps of this process have been the subject of theoretical investigations,[33,35] the whole catalytic cycle still remains unclear. A full understanding of the whole mechanism is thus of great interest in order to apprehend the most important parameters and therefore be able to take advantage of the nucleophilic character of η^1-allyl palladium complexes for the catalytic allylation of other electrophiles.

As illustrated in Scheme 2, all tridentate ligands used in the catalyzed allylation of aldehydes feature a central C-sp^2 carbon atom. Reasoning that the electronic nature of the central ligand (trans to the allyl moiety) would play a crucial role in the reactivity of these η^1-palladium allyl complexes, we launched a study aimed at evaluating the activity of an L∼P∼L pincer ligand. Earlier this decade, we developed a straightforward synthesis of tridentate S∼P∼S anionic ligands featuring a λ^5-phosphinine as central ligand and two ancillary phosphinosulfide groups. These new tridentate systems proved to be remarkable ligands for transition group metals (groups 7,[39] 9,[40,41] 10,[42,43] 11[44]) and even actinides (U^{IV}).[45] The synthesis of S∼P∼S complexes is presented in Scheme 3. Most interestingly, complexes of group 10 metals proved not only quite efficient in catalyzing C−C bond forming reactions, but also very robust. Thus a (S∼P∼S)−Pd complex was shown to be the best catalyst for the formation of arylboronic acids from pinacol borane and aryl iodides (TONs up to 76500).[42]

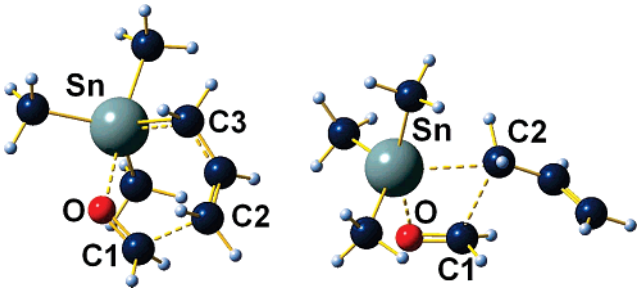

FIGURE 1. Views of the transition states $\mathbf{TS}_\gamma$ (left picture) and $\mathbf{TS}_\alpha$ (right picture) corresponding to the direct reaction of allyltrimethyltin with formaldehyde as given by DFT calculations. Most significant bond distances (Å) and angles (deg): $\mathbf{TS}_\gamma$: Sn−O, 2.37; Sn−C3, 2.33; O−C1, 1.26; C1−C2, 2.21; O−Sn−C3, 76.8. $\mathbf{TS}_\alpha$: Sn−O, 2.27; Sn−C2, 2.53; O−C1, 1.27; C1−C2, 2.20; O−Sn−C2, 77.0.

As will be seen, a parallel study of the catalytic activity of S∼P∼S and isoelectronic S∼C∼S palladium complexes as well as experiments run without catalyst prompted us to fully investigate the full catalytic cycle through DFT calculations. All the data lead to reconsider the involvement of η^1-allyl palladium pincer complexes in the electrophilic allylation of aldehydes and to propose a new mechanism.

Results and Discussion

1. Experimental Results. In order to establish a more accurate comparison between S∼C∼S and S∼P∼S systems, all our catalytic studies were carried out with catalysts **1** and **2**. A series of para-substituted benzaldehydes, namely *p*-nitrobenzaldehyde, *p*-bromobenzaldehyde, benzaldehyde, and *p*-tolualdehyde were reacted with catalytic amounts of **1** and **2** (Scheme 4).

All reactions were carried out in THF or $CHCl_3$, and the reaction time was set at 24 h. Both complexes proved to be active for this reaction with a low charge of catalyst (1.0 mol %). Furthermore their activities compare very well to those reported in the literature with palladium pincer complexes that feature a chloride ligand. Complex **2** exhibited a higher activity

(35) Solin, N.; Kjellgren, J.; Szabo, K. J. *J. Am. Chem. Soc.* **2004**, *126*, 7026−7033.
(36) Nakamura, H.; Iwama, H.; Yamamoto, Y. *J. Am. Chem. Soc.* **1996**, *118*, 6641−6647.
(37) Yao, Q. W.; Sheets, M. *J. Org. Chem.* **2006**, *71*, 5384−5387.
(38) Baber, R. A.; Bedford, R. B.; Betham, M.; Blake, M. E.; Coles, S. J.; Haddow, M. F.; Hursthouse, M. B.; Orpen, A. G.; Pilarski, L. T.; Pringle, P. G.; Wingad, R. L. *Chem. Commun.* **2006**, 3880−3882.
(39) Doux, M.; Mezailles, N.; Ricard, L.; Le Floch, P.; Vaz, P. D.; Calhorda, M. J.; Mahabiersing, T.; Hartl, F. *Inorg. Chem.* **2005**, *44*, 9213−9224.
(40) Doux, M.; Mezailles, N.; Ricard, L.; Le Floch, P. *Organometallics* **2003**, *22*, 4624−4626.
(41) Doux, M.; Ricard, L.; Le Floch, P.; Jean, Y. *Organometallics* **2005**, *24*, 1608−1613.
(42) Doux, M.; Mezailles, N.; Melaimi, M.; Ricard, L.; Le Floch, P. *Chem. Commun.* **2002**, 1566−1567.
(43) Doux, M.; Mezailles, N.; Ricard, L.; Le Floch, P. *Eur. J. Inorg. Chem.* **2003**, 3878−3894.
(44) Doux, M.; Ricard, L.; Le Floch, P.; Mezailles, N. *Dalton Trans.* **2004**, 2593−2600.
(45) Arliguie, T.; Doux, M.; Mezailles, N.; Thuery, P.; Le Floch, P.; Ephritikhine, M. *Inorg. Chem.* **2006**, *45*, 9907−9913.

TABLE 1. Catalytic Results of the Allylation of Aldehydes with Allyltributyltin[a]

entry	R-C_6H_5CO	catalyst	cocatalyst	solvent	temp	yield, %
1	pNO_2-C_6H_5CO	**1**	-	THF	RT	41
2	pBr-C_6H_5CO	**1**	-	THF	50 °C	66
3	pBr-C_6H_5CO	**1**	-	$CHCl_3$	50 °C	57
4	C_6H_6CO	**1**	-	$CHCl_3$	50 °C	30
5	pMe-C_6H_5CO	**1**	-	$CHCl_3$	50 °C	17
6	pNO2-C_6H_5CO	**2**	-	THF	RT	49
7	pBr-C_6H_5CO	**2**	-	$CHCl_3$	50 °C	94
8	C_6H_6CO	**2**	-	$CHCl_3$	50 °C	82
9	pMe-C_6H_5CO	**2**	-	$CHCl_3$	50 °C	50
10	pBr-C_6H_5CO	**1**	$AgBF_4$ (5.0 mol %)	THF	RT	83 (15)[b]
11	pBr-C_6H_5CO	**2**	AgBF4 (5.0 mol %)	THF	RT	78 (21)[b]

[a] All reactions were performed with 1 equiv of aldehyde and 1.2 equiv of allyltributyltin. 1.0 mol% catalyst was used. [b] Yields observed in the absence of silver tetrafluoroborate are given in parentheses.

TABLE 2. Results for the Noncatalyzed Allylation of Aldehydes with Allyltributyltin[a]

entry	R-C_6H_5CO	solvent	temp	yield, %
1	pNO_2-C_6H_5CO	THF	RT	8
2	pBr-C_6H_5CO	THF	RT	0
3	C_6H_6CO	THF	RT	0
4	pMe-C_6H_5CO	THF	RT	0
5	PNO_2-C_6H_5CO	THF	50 °C	42
6	pBr-C_6H_5CO	THF	50 °C	0
7	C_6H_6CO	THF	50 °C	0
8	pMe-C_6H_5CO	THF	50 °C	0
9	pNO_2-C_6H_5CO	toluene	110 °C	100
10	pBr-C_6H_5CO	toluene	110 °C	86
11	C_6H_6CO	toluene	110 °C	73
12	pMe-C_6H_5CO	toluene	110 °C	60

[a] All reactions were performed with 1 equiv of aldehyde and 1.2 equiv of allyltributyltin.

SCHEME 5. Energy Profile for the Condensation of Allyltrimethyltin with Formaldehyde

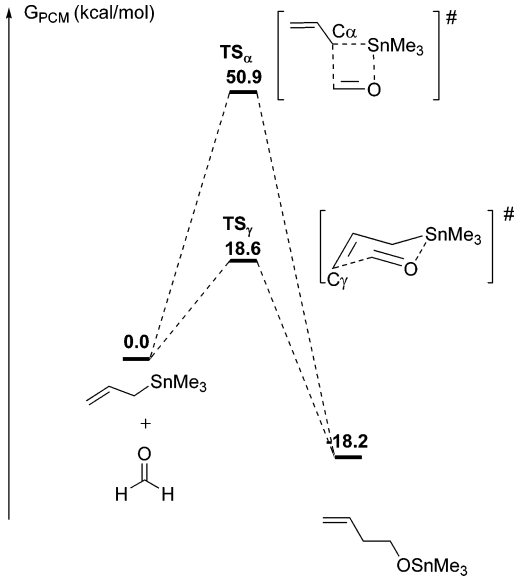

than phosphinine-based complex **1**. For example, *p*-bromobenzaldehyde is converted in 94% after 24 h at 50 °C when **2** is used as catalyst (1.0 mol %, entry 7). In the same conditions, complex **1** produces the desired product in 57% yield (entry 3). As reported previously, electron deficient aldehydes were more easily converted (compare entries 7, 8, and 9). Importantly, abstraction of the chloride ligand by silver tetrafluoroborate (5 mol % as cocatalyst) improves significantly the catalytic activity of both complexes (entries 10 and 11).[46] For instance, allylation

SCHEME 6. Energy Profile for the Noncatalyzed Allylation of Para-Substituted Benzaldehydes

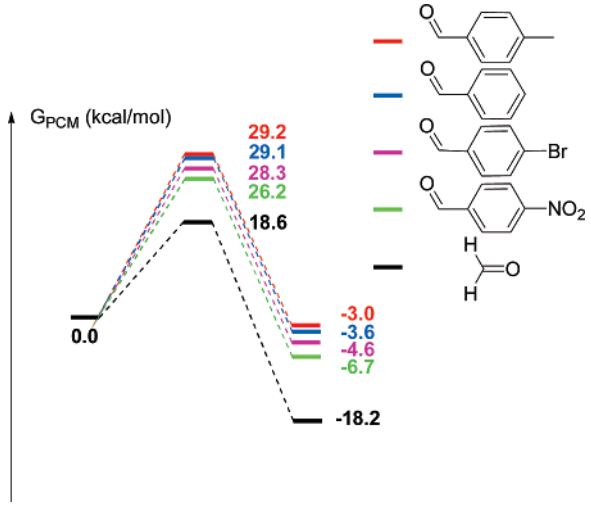

of *p*-bromobenzaldehyde with allyltributyltin reaches 83% in THF at room temperature after 24 h with 1.0 mol % complex **1** and 5.0 mol % $AgBF_4$, whereas it only reaches 15% in the absence of the silver salt. Under these conditions, better conversions are observed when complex **1** is employed, a result that may be attributed to the higher stability of the phosphinine-based complex upon activation by a silver salt.[47]

Although the noncatalyzed reaction was previously reported not to proceed, a reaction in absence of catalyst was performed for the most active substrate. Contrary to the earlier report, we found that the direct reaction between allyltributyltin and *p*-nitrobenzaldehyde afforded the corresponding alcohol with a moderate but significant yield (8%) after 24 h at room temperature. This result prompted us to investigate the noncatalyzed reaction in more detail. Allylation of a variety of commonly employed aldehydes was thus achieved under different experimental conditions (reaction times and temperatures). All these results are summarized in Table 2.

According to these results, it is clear that careful attention should be paid to the experimental conditions of the catalyzed version to avoid the competitive direct allylation and determine a proper catalytic activity, especially for electron deficient substrates (i.e., *p*-nitrobenzaldehyde). As expected for a nu-

(46) Control experiments indicated that no conversion is observed in the presence of 5.0 mol% $AgBF_4$ and in the absence of catalyst.

(47) Deactivation of tetrafluoroborate complex **II** has already been observed under catalytic conditions; see reference 35.

SCHEME 7. Two Proposed Mechanisms Accounting for the Palladium-Catalyzed Allylation of Aldehydes by Allyltin Derivatives

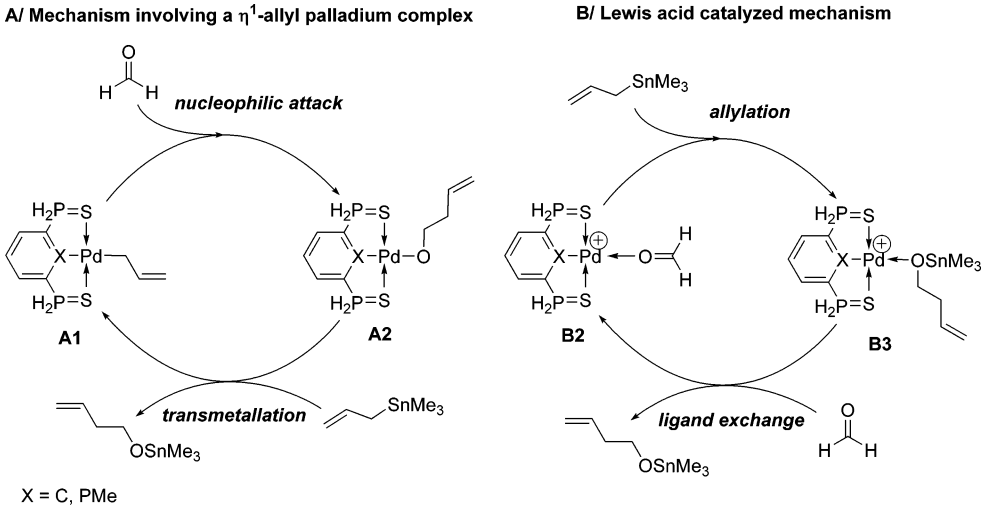

cleophilic allylation, electron deficient aldehydes react much faster than electron rich ones. For example, conversion of *p*-nitrobenzaldehyde into the homoallylic alcohol reaches 100% in toluene at 110 °C for 24 h. Under the same conditions, *p*-tolualdehyde is converted to 60%. Interestingly, these experimental results show that the overall electronic demand on the aldehyde is the same for the two mechanisms (catalyzed and noncatalyzed).

These results can be compared to results reported in the literature that present high TON for the palladium-catalyzed allylation. Indeed, Yao and co-workers reported on the remarkable catalytic activity of a [(Se∼C∼Se)Pd-OAc] pincer complex in the allylation of *p*-nitrobenzaldehyde. A conversion of 79.5% was obtained with 0.005 mol % catalyst in DMF at 40 °C after 96 h of reaction.[37] In our hands, under the same experimental conditions, the uncatalyzed reaction afforded the desired alcohol with a 53.0% conversion. All these results prompted us to reinvestigate the mechanism of this transformation. For this, a DFT study was carried out on the uncatalyzed as well as on the palladium-catalyzed process.

2. Mechanistic Investigations. 2.1. Computational Details. All calculations were carried out using the Gaussian 03 set of programs[48] with the B3PW91 functional,[49,50] the 6-31+G* basis set for all nonmetallic atoms (H, C, O, P, N, Cl, S), the lanl2dz[51] basis set for tin augmented with a d polarization function,[52] and the Hay−Wadt[51] basis set for palladium augmented with a f polarization function.[53] Further computational details are given in the Supporting Information. The structures of the intermediates and transition states were optimized without symmetry constraint. Transition states were identified by having one imaginary frequency in the Hessian matrix.

To take into account the role of the solvent, single point calculations were carried out on the optimized structures using

SCHEME 8. Energy Profile for the Nucleophilic Attack of the η^1-Allyl Palladium Complexes

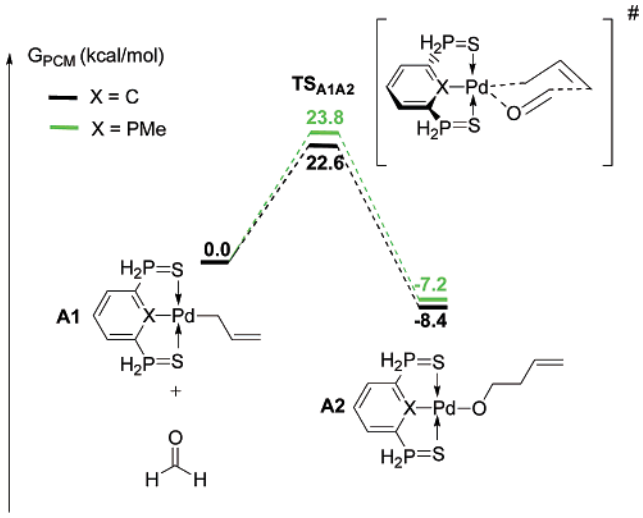

the Polarized Continuum Model (PCM),[54−57] THF being considered as the solvent. The catalytic reaction considered corresponds to a condensation; therefore, the entropic factor is not negligible, and energies reported in this article will include a gas-phase entropic correction (energies will be quoted as ΔG) as proposed recently by the group of Maseras.[58]

$$\Delta G = \Delta E_{PCM} + (\Delta G_{gas} - \Delta E_{SCF,gas})$$

2.2. Mechanism of the Noncatalyzed Reaction. Based on the experimental results (Table 2), the mechanism of the noncatalyzed reaction was first investigated. Two pathways were considered depending on which carbon atom (C_α or C_γ) of the

(48) Frisch, M. J. et al. Gaussian 03W (Revision C.02); Gaussian, Inc.: Pitsburgh PA, 2003.
(49) Becke, A. D. *J. Chem. Phys.* **1993**, *98*, 5648−5652.
(50) Perdew, J. P.; Wang, Y. *Phys. Rev. B.* **1992**, *45*, 13244−13249.
(51) Hay, P. J.; Wadt, W. R. *J. Chem. Phys.* **1985**, *82*, 299−310.
(52) Hollwarth, A.; Bohme, M.; Dapprich, S.; Ehlers, A. W.; Gobbi, A.; Jonas, V.; Kohler, K. F.; Stegmann, R.; Veldkamp, A.; Frenking, G. *Chem. Phys. Lett.* **1993**, *208*, 237−240.
(53) Ehlers, A. W.; Bohme, M.; Dapprich, S.; Gobbi, A.; Hollwarth, A.; Jonas, V.; Kohler, K. F.; Stegmann, R.; Veldkamp, A.; Frenking, G. *Chem. Phys. Lett.* **1993**, *208*, 111−114.
(54) Miertus, S.; Scrocco, E.; Tomasi, J. *Chem. Phys.* **1981**, *55*, 117−129.
(55) Cossi, M.; Barone, V.; Cammi, R.; Tomasi, J. *Chem. Phys. Lett.* **1996**, *255*, 327−335.
(56) Cossi, M.; Scalmani, G.; Rega, N.; Barone, V. *J. Chem. Phys.* **2002**, *117*, 43−54.
(57) Barone, V.; Improta, R.; Rega, N. *Theor. Chem. Acc.* **2004**, *111*, 237−245.
(58) Braga, A. A. C.; Ujaque, G.; Maseras, F. *Organometallics* **2006**, *25*, 3647−3658.

SCHEME 9. Transmetalation Pathways in the Stille-Coupling

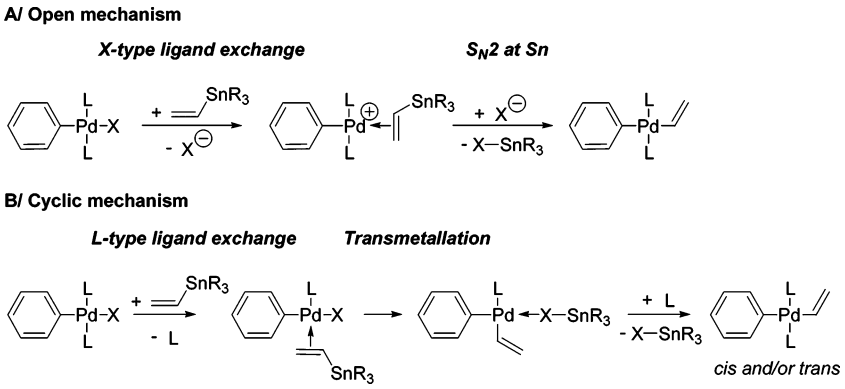

allyl moiety attacks the carbon of the aldehyde. Electrophilic attack at the C_γ position leads to a six-center transition state which adopts a chairlike conformation (**TS**$_\gamma$). This transition state was found to be much lower in energy than the four-center transition state resulting from the attack at C_α (**TS**$_\alpha$, $\Delta G^{\ddagger}_\alpha$ = 50.9 kcal/mol and $\Delta G^{\ddagger}_\gamma$ = 18.6 kcal/mol). Both transition states are presented in Figure 1, and representative bond distances and angles are collected in the corresponding figure caption. Formation of alkoxide-tin from formaldehyde and allyltrimethyltin is an exergonic process (ΔG = −18.2 kcal/mol, Scheme 5).

In order to validate this model mechanism, the noncatalyzed reaction was also computed with various aldehydes: *p*-nitrobenzaldehyde, *p*-bromobenzaldehyde, benzaldehyde, and *p*-tolualdehyde (Scheme 6). Geometries of the corresponding transition states were found to be relatively similar to those obtained with preliminary calculations using formaldehyde as reactant (**TS**$_\gamma$). However energies were significantly affected. Indeed, electron-withdrawing groups on the para position favor both the kinetics and the thermodynamics of the reaction. These results yielded the following reactivity scale: *p*-nitrobenzaldehyde ≫ *p*-bromobenzaldehyde > benzaldehyde ≥ *p*-tolualdehyde(>: reacts faster than). Note that this reactivity scale nicely compares with experimental results (Table 2). Moreover, the computed energetic barriers are consistent with reactions proceeding at ambient temperature or with mild heating (26.2 kcal/mol < $\Delta G^{\ddagger}$ < 29.2 kcal/mol).

These values, for a given substrate, set the upper limit for the palladium-catalyzed process since a catalytic pathway must

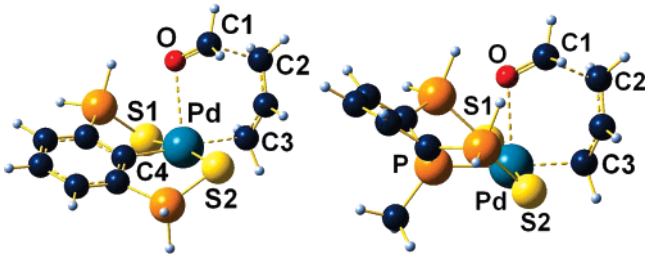

FIGURE 2. Views of the transition states **TS**$_{A1A2,SCS}$ (left picture) and **TS**$_{A1A2,SPS}$ (right picture) corresponding to the nucleophilic attack of the η^1-allyl palladium complexes as given by DFT calculations. Most significant bond distances (Å) and angles (deg): **TS**$_{A1A2,SCS}$: C1−O, 1.27; C1−C2, 1.91; Pd−O, 2.66; Pd−C3, 2.22; Pd−C4, 2.04; Pd−S1, 2.42; Pd−S2, 2.41; O−Pd−C3, 87.6; C3−Pd−C4, 177.4; S1−Pd−S2, 170.8. **TS**$_{A1A2,SPS}$: C1−O, 1.27; C1−C2, 1.92; Pd−O, 2.66; Pd−C3, 2.18; Pd−P, 2.31; Pd−S1, 2.40; Pd−S2, 2.41; O−Pd−C3, 94.4; C3−Pd−P, 177.0; S1−Pd−S2, 174.9.

SCHEME 10. Energy Profile of the Alcoholate to Allyltin Ligand Exchange

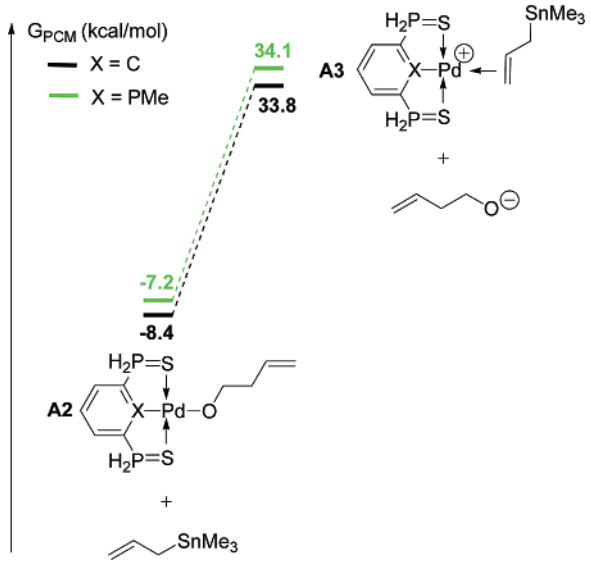

be more favorable than the noncatalyzed transformation. The rate-determining steps for the catalyzed mechanism therefore must involve lower activation energies than those found for the noncatalyzed mechanism (18.6 kcal/mol in the case of formaldehyde).

Further calculations then focused on the determination of the catalyzed pathway. Two model ligands of the phosphinine-based S∼P∼S (**1**) and the aryl S∼C∼S (**2**)-based palladium complexes were considered. To save computational time, phenyl groups were replaced by hydrogen atoms and the butyl group on the phosphorus atom was replaced by a methyl group. On the other hand, allyltrimethyltin was considered in place of allyltributyltin, and formaldehyde was used as a model of the carbonyl reactant. Energies corresponding to the S∼C∼S and S∼P∼S-based palladium catalysts will be labeled by a SCS (i.e.: ΔG_{SCS}) and SPS index, respectively.

Two mechanistic pathways were investigated: a first mechanism involving the transient formation of η^1-allyl complexes proposed in literature (Scheme 7, A),[34,35] and a mechanism in which the metal center acts as a Lewis acid as suggested by the occurrence of the noncatalyzed reaction (Scheme 7, B). These two competing mechanisms are summarized in the following scheme (Scheme 7).

2.3. Mechanism Involving an η^1-Allyl Palladium Complex. The first mechanism relies on the peculiar reactivity of η^1-allyl

SCHEME 11. Energy Profile of the Concerted Transmetalation Step

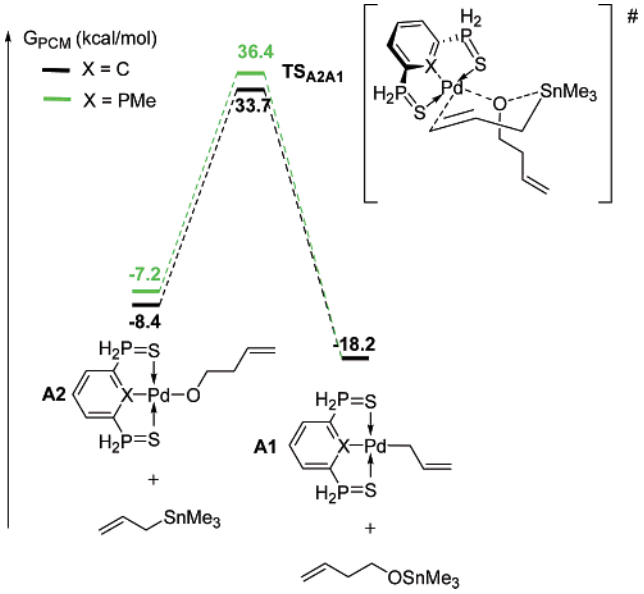

palladium complexes in which the allyl moiety exhibits a nucleophilic character. It proceeds in two steps (Scheme 7, A): a nucleophilic attack of the η^1-allyl palladium complex **A1** followed by a transmetalation step allowing the regeneration of **A1** from **A2**. Both steps of this mechanism were computed. First, nucleophilic attack of the allyl-metal occurs at the Cγ position and yields the corresponding alcoholate which remains coordinated to the metal center (**A2**, Scheme 8). The overall transformation was found to be exergonic ($\Delta G_{A1A2,SCS} = -8.4$ kcal/mol and $\Delta G_{A1A2,SPS} = -7.2$ kcal/mol). The six-membered palladacycle Pd−C−C−C−O in $\mathbf{TS_{A1A2}}$ adopts a chairlike conformation which is close to what is observed for $\mathbf{TS}_\gamma$. The palladium atom lies in a square-based pyramid in which the tridentate (S∼X∼S) ligand and the allyl group form the square base (Figure 2). With both ligands (S∼C∼S and S∼P∼S) this step requires an activation energy at least 4.0 kcal/mol higher than for the noncatalyzed transformation ($\Delta G^{\ddagger}_{A1A2,SCS} = 22.6$ kcal/mol, $\Delta G^{\ddagger}_{A1A2,SPS} = 23.8$ kcal/mol vs $\Delta G^{\ddagger}_{\gamma} = 18.6$ kcal/mol).[59]

The second step of this first mechanism is a transmetalation process which accounts for the regeneration of the η^1-allyl complex **A1** and the concomitant release of the reaction product. Transmetalation of an organic fragment from tin to palladium is a key step in many catalytic processes.[28,60−62] For example, in the Stille reaction, a palladium complex catalyzes the cross-coupling between an aryl halide (or triflate) and an arylstannane. The mechanism of this reaction has been widely investigated and has been shown to proceed *via* three steps, namely (i) an oxidative addition of a palladium(0) complex to the aryl halide, (ii) followed by a tin-to-palladium transmetalation, and (iii) a final reductive elimination which affords the desired bis-aryl product and regenerates the 14VE PdL_2 catalytic species.[28] Though both the oxidative addition and the reductive elimination

SCHEME 12

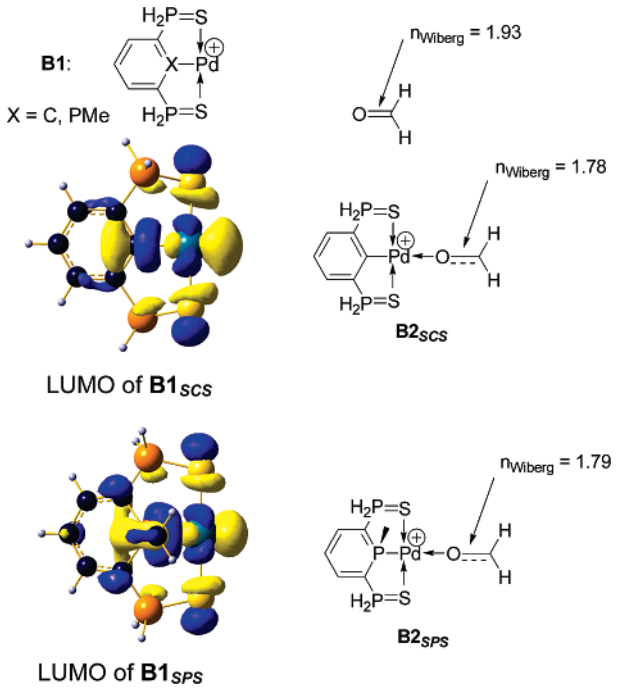

steps have been early established and understood, the precise mechanism of the transmetalation step has been the subject of many debates. After thorough experimental and theoretical studies, two mechanisms were finally retained: an open mechanism and a cyclic mechanism (Scheme 9).[28,63−67] The open mechanism was shown to involve two steps (Scheme 9, A): the vinylstannane first displaces an X-type ligand in the coordination sphere of the metal. The proper transfer of the vinyl group occurs then *via* a S_N2 attack of the X^- anion at the tin center. In this process, the controlling step is the displacement of an X-type ligand and is therefore favored when X is a triflate anion (instead of an halide). The cyclic mechanism involves an L-type ligand exchange followed by a transmetalation (involving a cyclic transition state) that controls the kinetics of the reaction (see Scheme 9, B).

At first sight, two analogous mechanisms can be proposed for the transformation of **A2** to **A1**. The open mechanism requires the displacement of the alcoholate ligand in **A2** by the allylstannane (behaving as a metallo-ligand) that would afford the cationic complex **A3**. Whatever the exact mechanism of this ligand exchange (associative or dissociative), this step is highly endergonic, **A3** lying at least 41.3 kcal/mol higher than **A2** (Scheme 10). The subsequent S_N2 attack of the alcoholate at the tin center was therefore not computed.

The cyclic mechanism was then envisioned. However, the κ^3-coordination mode of the tridentate S∼X∼S ligand precludes the L-type ligand exchange. As a consequence, the cyclic mechanism can only proceed in a concerted manner *via* a

(59) Note that the first step of this mechanism has already been described in the literature with pincer palladium complexes (but not compared to the noncatalyzed process); energies and geometries were found to be consistent with those reported. See refs 33 and 35.

(60) Suzuki, A. *J. Organomet. Chem.* **1999**, *576*, 147−168.
(61) Suzuki, A. *J. Organomet. Chem.* **2002**, *653*, 83−90.
(62) Miyaura, N.; Suzuki, A. *Chem. Rev.* **1995**, *95*, 2457−2483.
(63) Casares, J. A.; Espinet, P.; Salas, G. *Chem. Eur. J.* **2002**, *8*, 4843−4853.
(64) Cotter, W. D.; Barbour, L.; McNamara, K. L.; Hechter, R.; Lachicotte, R. J. *J. Am. Chem. Soc.* **1998**, *120*, 11016−11017.
(65) Nova, A.; Ujaque, G.; Maseras, F.; Lledos, A.; Espinet, P. *J. Am. Chem. Soc.* **2006**, *128*, 14571−14578.
(66) Nilsson, P.; Puxty, G.; Wendt, O. F. *Organometallics* **2006**, *25*, 1285−1292.
(67) Ricci, A.; Angelucci, F.; Bassetti, M.; Lo Sterzo, C. *J. Am. Chem. Soc.* **2002**, *124*, 1060−1071.

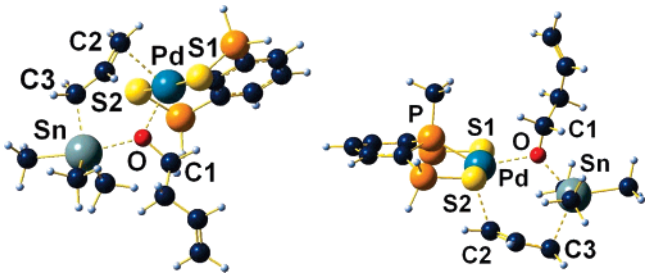

FIGURE 3. Views of the transition states $\mathbf{TS_{A2A1,SCS}}$ (left picture) and $\mathbf{TS_{A2A1,SPS}}$ (right picture) corresponding to the transmetalation step as given by DFT calculations. Most significant bond distances (Å) and angles (deg): $\mathbf{TS_{A2A1,SCS}}$: Pd−O, 2.38; Pd−C2, 2.54; Pd−S1, 2.38; Pd−S2, 2.39; C3−Sn, 2.23; Sn−O, 2.33; O−C1, 1.39; C2−Pd−O, 96.7; S1−Pd−S2, 176.1. $\mathbf{TS_{A2A1,SPS}}$: Pd−O, 2.36; Pd−C2, 2.69; Pd−S1, 2.39; Pd−S2, 2.40; P−Pd, 2.23; C3−Sn, 2.34; Sn−O, 2.14; O−C1, 1.41; C2−Pd−O, 92.6; S1−Pd−S2, 175.4.

SCHEME 13. Energy Profile for the Formation of Complex B2

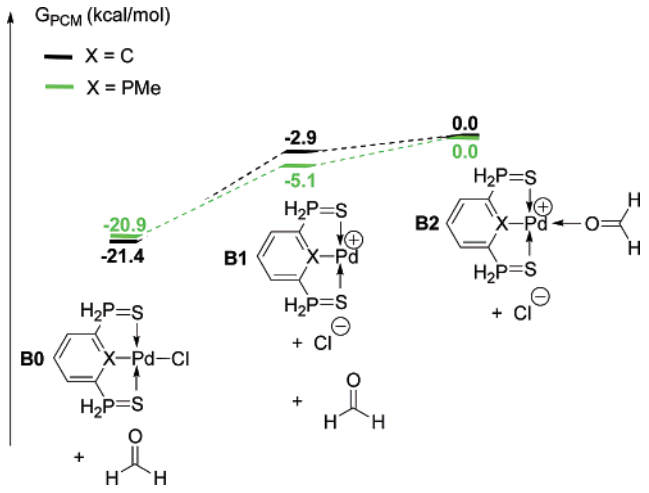

pentacoordinated palladium center. In fact, $\mathbf{TS_{A2A1}}$ adopts a chairlike conformation, and the geometry around the palladium center is close to a trigonal bipyramid with the two sulfur atoms occupying the axial positions (Figure 3). This step was found to be exergonic ($\Delta G_{A2A1,SCS} = -9.8$ kcal/mol, $\Delta G_{A2A1,SPS} = -11.0$ kcal/mol, Scheme 11) but requires a large activation energy ($\Delta G^{\ddagger}_{A2A1,SCS} = 42.1$ kcal/mol, $\Delta G^{\ddagger}_{A2A1SPS} = 43.6$ kcal/mol).

To summarize, this first mechanism proceeds *via* two different steps. First, the η^1-allyl palladium complex attacks the electrophilic aldehyde at the C_γ position. This attack was found to be significantly less favorable than the direct coupling between formaldehyde and allyltrimethyltin. The regeneration of the η^1-allyl palladium complex occurs then, *via* a transmetalation step, which is very energy demanding whatever the pathway envisioned (open or cyclic). Although very interesting from a mechanistic point of view, both steps of this first mechanism were shown to require higher activation energies than the uncatalyzed process.

2.4. Lewis Acid Mechanism. A mechanism in which the metal center acts as a Lewis acid has already been suggested in literature for the allylation of aldehydes by allyltin derivatives and would account for the existence of non-palladium-based catalysts (Zn, Zr, Ag, etc.).[68−77] In the case of palladium pincer complexes used in this process, the Lewis acid moiety would

SCHEME 14. Energy Profile of the Lewis Acid-Promoted Allylation Step

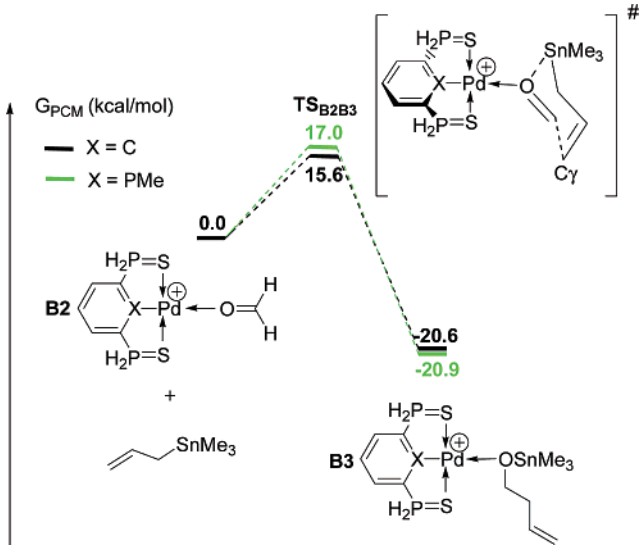

SCHEME 15. Energy Profile of the Ligand Exchange

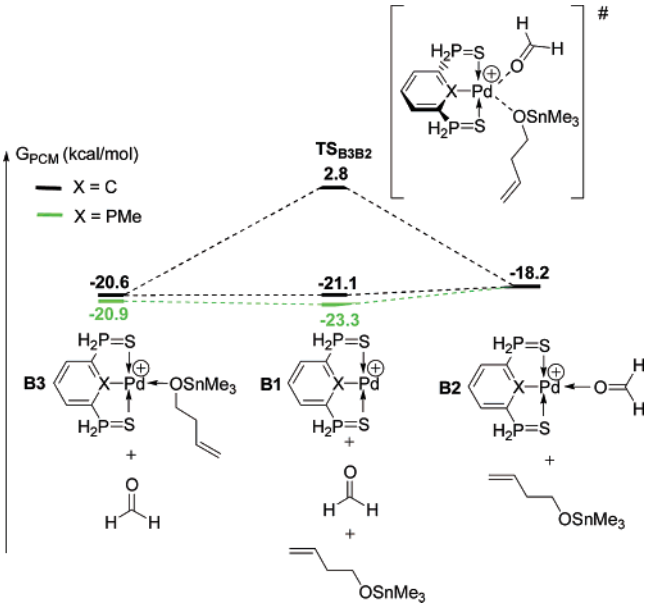

consist in a cationic PdL_3^+ fragment. Indeed pincer ligands impose a T-shape geometry for the PdL_3^+ complex (**B1**) which therefore possesses a low lying vacant $d_{x^2-y^2}$ orbital at the metal

(68) Denmark, S. E.; Fu, J. P. *Chem. Rev.* **2003**, *103*, 2763−2793.
(69) Yanagisawa, A.; Nakashima, H.; Ishiba, A.; Yamamoto, H. *J. Am. Chem. Soc.* **1996**, *118*, 4723−4724.
(70) Cozzi, P. G.; Orioli, P.; Tagliavini, E.; UmaniRonchi, A. *Tetrahedron Lett.* **1997**, *38*, 145−148.
(71) Imai, Y.; Zhang, W. B.; Kida, T.; Nakatsuji, Y.; Ikeda, I. *J. Org. Chem.* **2000**, *65*, 3326−3333.
(72) Kwong, H. L.; Lau, K. M.; Lee, W. S.; Wong, W. T. *New J. Chem.* **1999**, *23*, 629−632.
(73) Bedeschi, P.; Casolari, S.; Costa, A. L.; Tagliavini, E.; Umaironchi, A. *Tetrahedron Lett.* **1995**, *36*, 7897−7900.
(74) Casolari, S.; Cozzi, P. G.; Orioli, P.; Tagliavini, E.; UmaniRonchi, A. *Chem. Commun.* **1997**, 2123−2124.
(75) Kurosu, M.; Lorca, M. *Tetrahedron Lett.* **2002**, *43*, 1765−1769.
(76) Hanawa, H.; Kii, S.; Asao, N.; Maruoka, K. *Tetrahedron Lett.* **2000**, *41*, 5543−5546.
(77) Motoyama, Y.; Okano, M.; Narusawa, H.; Makihara, N.; Aoki, K.; Nishiyama, H. *Organometallics* **2001**, *20*, 1580−1591.

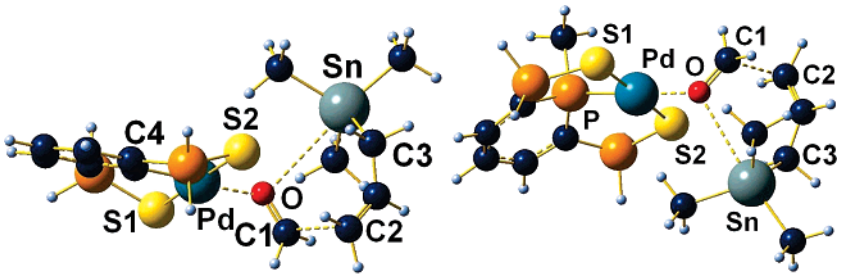

FIGURE 4. Views of the transition states $\mathbf{TS_{B2B3,SCS}}$ (left picture) and $\mathbf{TS_{B2B3,SPS}}$ (right picture) corresponding to the reaction of allyltrimethyltin with formaldehyde with palladium pincer complexes acting as Lewis acids as given by DFT calculations. Most significant bond distances (Å) and angles (deg): $\mathbf{TS_{B2B3,SCS}}$: Pd−O, 2.13; Pd−S1, 2.38; Pd−S2, 2.38; Pd−C4, 1.99; Sn−O, 3.42; Sn−C3, 2.25; C1−C2, 2.25; C1-O, 1.26; C4-Pd−C1, 176.9; S1−Pd−S2, 177.3. $\mathbf{TS_{B2B3,SPS}}$: Pd−O, 2.16; Pd−S1, 2.39; Pd−S2, 2.39; Pd−P, 2.22; Sn−O, 3.26; Sn−C3, 2.24; C1−C2, 2.28; C1-O, 1.25; P−Pd−C1, 176.5; S1−Pd−S2, 176.3.

center (Scheme 12). Coordination of the aldehyde on the T-shaped PdL_3^+ fragment results in the formation of a square planar complex (**B2**) in which the aldehyde is activated as shown by the decrease of the carbon−oxygen Wiberg Bond Index (1.78 in $\mathbf{B2_{SCS}}$ and 1.79 in $\mathbf{B2_{SPS}}$ vs 1.93 in free formaldehyde).

The formation of complex **B1** requires the decoordination of the chloride anion from the precatalyst complex **B0** (Scheme 13). This dissociation step was found to be endergonic ($\Delta G_{B0B1,SCS}$ = 18.4 kcal/ mol, $\Delta G_{B0B1,SPS}$ = 15.8 kcal/mol). This step does not depend on the nature of the aldehyde, and thus its thermodynamics should be compared to that of the noncatalyzed transformation on real systems (benzaldehyde derivatives in place of formaldehyde) which range from 26.2 to 29.2 kcal/mol. Generation of the Lewis acid **B1** is therefore conceivable under the catalytic conditions.

After formation of the active complex **B2**, the Lewis acid mechanism proceeds in two steps (Scheme 7, B), namely a Lewis acid-promoted allylation yielding the desired coupling product coodinated to the palladium center (**B3**) and a ligand exchange (Scheme 14). The allylation step is close to the mechanism proposed for the direct conversion, the palladium center being coordinated to the oxygen atom (Figure 4). We found that the activation of the aldehyde provided by coordination to the cationic fragment lowers the activation energy required for this step by 3.0 kcal/mol in the case of $\mathbf{TS_{B2B3,SCS}}$ and by 1.6 kcal/mol in the case of $\mathbf{TS_{B2B3,SPS}}$ ($\Delta G^{\ddagger}_{B2B3,SCS}$ = 15.6 kcal/mol, $\Delta G^{\ddagger}_{B2B3,SPS}$ = 17.0 kcal/mol). This allylation step yields an adduct between the cationic pincer and the oxygen atom of the formed product which increases the exergonicity of the reaction by 2.4 kcal/mol for $\mathbf{B3_{SCS}}$ and by 2.7 kcal/mol for $\mathbf{B3_{SPS}}$ ($\Delta G_{\mathbf{B2B3,SCS}}$ = −20.6 kcal/mol, $\Delta G_{\mathbf{B2B3,SPS}}$ = −20.9 kcal/mol).

The next step of the process involves a ligand exchange on the palladium center of product of the reaction for formaldehyde (Scheme 15). Two pathways may account for this step depending on whether it occurs *via* an associative mechanism (with a penta-coordinated palladium center as transition state) or a dissociative mechanism (with a tricoordinated palladium center as intermediate). A transition state corresponding to an associative pathway could be located on the potential energy surface only in the case of the S∼C∼S complex ($\mathbf{TS_{B3B2,SCS}}$, Figure 5). This ligand exchange requires an activation energy of $\Delta G^{\ddagger}_{B3B2,SCS}$ = 23.4 kcal/mol. On the other hand, we found that a dissociative pathway is much more favorable, the pincer palladium complex (**B1**) lying slightly lower in energy than the adduct **B3** ($\Delta G_{B3B1,SCS}$ = −0.5 kcal/mol, $\Delta G_{B3B1,SPS}$ = −2.4 kcal/mol). Subsequent coordination of the aldehyde results in

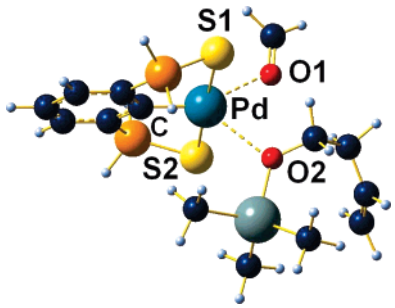

FIGURE 5. View of the transition state $\mathbf{TS_{B32B2,SCS}}$ ligand exchange between the formaldehyde and the reaction product as given by DFT calculations. Most significant bond distances (Å) and angles (deg): $\mathbf{TS_{B3B2,SCS}}$: Pd−O1, 2.42; Pd−O2, 2.62; Pd−S1, 2.37; Pd−S2, 2.38; Pd−C, 1.98; O1-Pd−O2, 74.5; O1-Pd−C, 151.2; O2-Pd−C, 134.2; S1−Pd−S2, 177.0.

the formation of complex **B2** in which the electrophilicity of the substrate is enhanced. This ligand exchange was found to be slightly endergonic ($\Delta G_{B3B2,SCS}$ = 2.4 kcal/mol, $\Delta G_{B3B2,SPS}$ = 2.7 kcal/mol).

Overall this new mechanism involves two steps: a Lewis acid-promoted allylation followed by a ligand exchange which proceeds *via* a dissociative pathway. The Lewis acid promoted allylation turns out to be the rate-determining step and, on the whole, this mechanism fits the requirement of an overall energy barrier lower than the one required for the noncatalyzed pathway. The electronic demand on the aldehyde is therefore the same for this mechanism and the noncatalyzed mechanism, as expected from experimental results (see Tables 1 and 2). Moreover cationic (S∼C∼S)Pd^+ fragment ($\mathbf{B1_{SCS}}$) appears to be a better Lewis acid than the analogous (S∼P∼S)Pd^+ fragment ($\mathbf{B1_{SPS}}$), thus leading to a lower energy barrier for the rate-determining allylation step. This computed result is in complete agreement with the experimental results showing complex **2** as a more active catalyst than **1**. This mechanism also nicely accounts for the role played by silver salts on the kinetics of this reaction: trapping the chloride ligand obviously favors the formation of the active species **B2**.

Comparison with Literature Results. The scope of this theoretical study was extended to two representative complexes proposed in literature. We chose to study the (Se∼C∼Se)PdX complex **III** which was shown to be an efficient catalyst for the allylation of aldehydes with allyltributyltin and the bis-carbene complex **V** which presents a low activity in this reaction. Allyltrimethyltin was considered in place of allyltribultin, formaldehyde was considered as a model of the aldehydes

SCHEME 16. Energy Profile of the Allylation Step in the Case of Complexes Described in the Literature

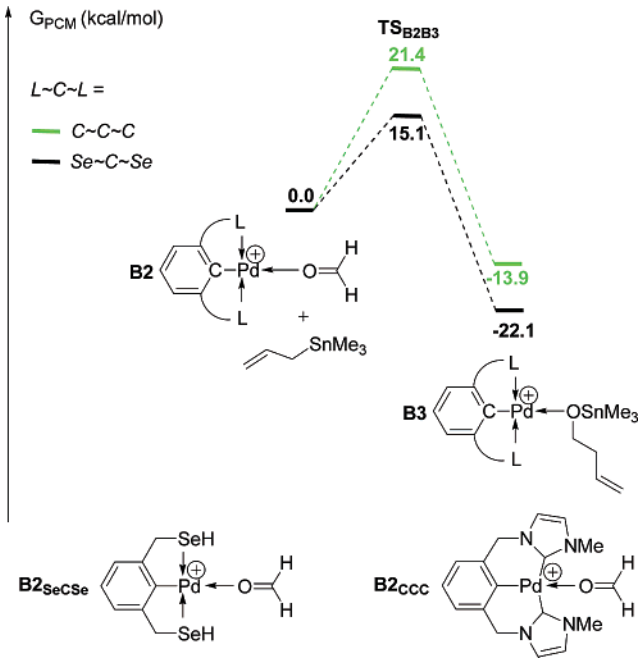

reactant, and phenyl groups on complex **III** were replaced by hydrogen atoms.

The Lewis acid-promoted allylation step was computed for these two complexes (Scheme 16). The activation energy with the Se∼C∼Se complex compares with barriers obtained for the S∼X∼S model complexes ($\Delta G^{\ddagger}_{B2B3,SeCSe} = 15.1$ kcal/mol vs $\Delta G^{\ddagger}_{B2B3,SPS} = 17.0$ kcal/mol and $\Delta G^{\ddagger}_{B2B3,SCS} = 15.6$ kcal/mol) which is in line with their respective activities. A larger activation energy was found for the bis-carbene complex, with $\Delta G^{\ddagger}_{B2B3,CCC} = 21.8$ kcal/mol. This energy is even higher that the one required for the noncatalyzed reaction ($\Delta G^{\ddagger}_{\gamma} = 18.6$ kcal/mol). The use of strong σ-donor ligands therefore results in a decrease of the Lewis acidity of the catalyst and in a concomitant lower catalytic activity.

Conclusion

η^1-Allyl palladium complexes have attracted much attention because of their nucleophilic character which can be exploited to extend the synthetic scope of allylpalladium species to electrophilic reagents. The electrophilic allylation of aldehydes with allylstannanes catalyzed by palladium pincer complexes was proposed as a model reaction to illustrate the feasibility of this strategy. In this study we have shown that pincer palladium complexes featuring S∼P∼S and a S∼C∼S substitution schemes are efficient catalysts for the electrophilic allylation of aldehydes using allylstannanes. The S∼C∼S palladium complex **2** exhibits a higher activity than the S∼P∼S palladium complex **1**, and both catalysts showed an increased activation in the presence of silver salts.

The full mechanism of this transformation was studied in detail by means of DFT calculations. Two pathways were explored: the commonly proposed mechanism involving η^1-allyl palladium intermediates and a Lewis acid-promoted mechanism. Both of these mechanisms were compared to the direct transformation that was shown experimentally to occur under mild conditions.

It was shown that, while the attack of an η^1-allyl palladium onto an aldehyde might be consistent with the experimental conditions, it requires a higher energetic demand than the one needed for the noncatalyzed transformation. Moreover, the transmetalation step following the electrophilic attack was found to be much disfavored on energetic grounds, definitely discarding this type of mechanism for this transformation. On the other hand, a cationic (S∼X∼S)Pd^+ fragment can form from the (S∼X∼S)PdCl complexes under the experimental conditions, especially if silver salts are added. This (S∼X∼S)Pd^+ species is an excellent Lewis acid able to activate the aldehyde toward a nucleophilic attack. The activation energy necessary to promote the allylation is thus lowered compared to the noncatalyzed transformation. The energetic profile of this reaction suggests a higher activity for the S∼C∼S ligand compared to the S∼P∼S ligand, in good agreement with the experimental result. This profile also accounts for the different activities observed in literature for electron rich and electron deficient catalysts. In the light of these results, we can conclude that this transformation does not involve η^1-allyl palladium intermediates but proceeds *via* a Lewis acid-based pathway.

Experimental Section

Palladium-Catalyzed Allylation of Aldehydes by Pincer Complex Catalysts. Representative procedure for the allylation of *p*-bromobenzaldehyde with allyltributyltin in the presence of complex **1**: A dried Schlenk was charged with *p*-bromo benzaldehyde (92.5 mg, 0.5 mmol), complex **1** (4.4 mg, 0.0050 mmol, 1.0 mol %), and THF (0.5 mL) under nitrogen. Allyl tributyltin (186μL, 0.6 mmol) was then added *via* syringe. The resulting solution was stirred at the desired temperature for 24 h. Thereafter the reaction mixture was evaporated, diluted into water, and extracted with ether. The organic layer was separated, washed with brine, dried (Na_2SO_4), and concentrated. The crude product was then purified by flash column chromatography (hexanes/EtOAc) to give the homoallylic alcohol as a colorless oil. The NMR data obtained for the coupling products are in agreement with the corresponding literature.[37,78]

Acknowledgment. The CNRS, the Ecole Polytechnique and the IDRIS (for computer time, project n°071616) are thanked for supporting this work.

Supporting Information Available: General remarks on the experimental section; computed Cartesian coordinates, SCF energies, thermochemistry and PCM energies, three lower frequenies of all theoretical structures, and complete reference 48. This material is available free of charge *via* the Internet at http://pubs.acs.org.

JO070467T

(78) Shen, K. H.; Yao, C. F. *J. Org. Chem.* **2006**, *71*, 3980−3983.